DYNAMICS OF METAL ELECTRON EXCITATION IN MOLECULAR DIPOLE-SURFACE COLLISIONS

Z. KIRSON

Department of Physical Chemistry and the Fritz Haber Research Center for Molecular Dynamics, Hebrew University, Jerusalem 91904, Israel
and
Department of Chemistry, Tel Aviv University, Tel Aviv 69978, Israel

R.B. GERBER

Department of Physical Chemistry and the Fritz Haber Research, Center for Molecular Dynamics, Hebrew University, Jerusalem 91904, Israel

A. NITZAN

Department of Chemistry, Tel Aviv University, Tel Aviv 69978, Israel

and

M.A. RATNER

Department of Chemistry, Northwestern University, Evanston, Illinois 60201, USA

Electron–hole pair excitations in low energy collisions of dipolar molecules with metal surface are studied in the framework of one-dimensional independent electron model. The motion of the incoming (rigid) molecule is treated classically and is coupled to the electron dynamics, which is treated quantum mechanically through the timedependent self-consistent field (TDSCF) approximation. Model calculations were carried out for NO and HCl molecules colliding with surface of Li and Al. The average fraction of collision energy converted to electron–hole pair excitation $\langle \Delta E \rangle / E$ and the probability for trapping due to this process were evaluated for collision energies in the range 0.01–10 eV. The effects of the pure dipolar electron–molecule interaction is compared to that of the short range interaction. It is concluded that the (screened) long range dipolar part of the electron–molecule interaction can play an important role in the collisional energy transfer between dipolar molecules and metal surfaces.

1. Introduction

Electron–hole pair excitation in atom–metal surface collisions has been the subject of several recent studies [1]. In previous work [1f] we have described a

quantum wavepacket approach to this problem. This approach is based on the independent electron model and on the time dependent self consistent field (TDSCF) approximation for treating the coupling between the motion of the electrons and the incoming atom. The TDSCF equation for the metal electron is solved using a time dependent variational procedure and a Gaussian wavepacket as a trial function. We have applied this method to the calculation of energy transfer due to electron–hole pair excitation in low energy collisions of hydrogen, helium and argon atoms with a Lithium surface. In the present article we use the same method to estimate the role played by the metal electrons in collisional energy transfer for a molecule–metal surface collision processes where the molecule is characterized by a permanent dipole moment. As specific examples we present results for collisions of HCl and NO molecules with Li and Al surfaces. We believe such theoretical and experimental studies to be of importance because the difference between collisional energy transfer processes involving polar and non-polar molecules is expected to provide indications to establish the relative role played by the metal electrons and the photons in such encounters.

This paper is organized as follows. In section 2 we define our model and in section 3 we review the TDSCF variational wavepacket approach. In section 4 we present the results for the electron–hole contribution to accommodation and sticking in NO and HCl collisions with Li and Al surfaces. Our results are analyzed and discussed in section 5.

2. The model

The metal is represented by a system of independent free electrons in a one-dimensional semi-infinite box defined over the negative half of the x axis. Even though we perform our dynamical calculation in a one-dimensional framework, we use parameters which characterize the given three-dimensional metal – its Fermi energy $\mathscr{E}_F$, the work function W and the electron density per unit volume (the latter is sometimes expressed in terms of $r_s = (3\rho/4\pi)^{1/3}$). The electronic wavefunctions are expanded in terms of the eigenfunctions of a particle subject to a potential field defined by

$$
V(x) = \begin{cases} 0 & \text{for} \quad x < 0, \\ W + \mathscr{E}_F & \text{for} \quad x > 0. \end{cases}
\tag{1}
$$

The metal is further characterized by its temperature T which determines the occupation probability of a state of energy

$$
f_T(\mathscr{E}) = \left\{ 1 + \exp\left[(\mathscr{E} - \mathscr{E}_F)/k_B T \right] \right\}^{-1}.
\tag{2}
$$

The parameters $\mathscr{E}_F$, W and r_s used in the calculations reported here for Li and Al are given in table 1.

The electron molecule interaction potential at large distances was taken to be the screened Coulomb potential between a point dipole and the metal electron. For this purpose we have adopted the simple screening theory of Newns [2] which is based on the linearized Thomas–Fermi approximation. Although more elaborate surface screening theories are available, we expect the linearized Thomas–Fermi approximation to be sufficient for the present crude calculations. Newns gives the following results for the potential at a point (R, x, φ) induced by a point charge Q located outside the metal at the point $R = 0$, $x = x_A$ (cylindrical coordinates are used with the normal from the source to the surface being the cylinder axis):

$$V(x) = Q\left[R^2 + (x - x_A)^2 \right]^{-1/2} + \int_0^\infty dk\, J_0(kR)\, e^{-kx} f(k), \quad \text{for} \quad x > 0,$$

$$V(x) = \int_0^\infty dk\, J_0(kR)\, \exp\left[(k^2 + \lambda^2)^{1/2} x \right] g(k), \qquad \text{for} \quad x < 0, \tag{3}$$

$$\tag{4}$$

where

$$f(k) = -Q\, e^{-kx_0} \left[\frac{k}{\lambda} - \left(1 + \frac{k^2}{\lambda^2} \right)^{1/2} \right]^2, \tag{5}$$

$$g(k) = -2Q\frac{k}{\lambda} e^{-kx_0} \left[\frac{k}{\lambda} - \left(1 + \frac{k}{\lambda} \right)^{1/2} \right], \tag{6}$$

and where λ^{-1} is the Thomas–Fermi screening length

$$\lambda = \left[4\pi e^2 g(\mathscr{E}_F) \right]^{1/2}, \tag{7}$$

e being the electron charge and $g(\mathscr{E}_F)$ the electronic density of states per unit volume at the Fermi level. The corresponding results for a dipole μ are obtained by taking the derivatives of eqs. (3) and (4) with respect to x and replacing Q by μ everywhere. To facilitate our computation we have fitted, with a very good accuracy, the result of this computation to the following

Table 1

Parameters for Li and Al; $\mathscr{E}_F$, W, r_s, a and λ are the Fermi energy, work function, the electron density parameter $r_s = (3\rho/4\pi)^{1/3}$, the lattice constant and the Thomas–Fermi screening length respectively

	$\mathscr{E}_F$ (eV)	W (eV)	r_s (a.u.)	a (a.u.)	λ (a.u.)
Li	11.70	2.38	3.25	6.6	0.854
Al	4.74	4.25	2.07	7.7	1.08

simple forms

$$V_{Ae}(x, x_A) = \begin{cases} \dfrac{\mu}{(x_A - x)^2}(1 - C_1 e^{-C_2 x}), & \text{for } x > 0 \quad \text{(vacuum)}, \\[2em] \pm(1 - C_1)\dfrac{\mu}{x_A^2}e^{C_3 x}, & \text{for } x < 0 \quad \text{(metal)}. \end{cases} \tag{8}$$

The parameters C_1, C_2 and C_3 were fitted so that V_{Ae} is the best fit to V of eqs. (3) and (4). The sign depends on whether the dipole is oriented with its positive side facing the metal or facing the other way. The $x < 0$ form of $V(x)$ was taken as the potential felt by an electron at x due to the molecular dipole at x_A. Values of the parameters C_1 and C_3 which correspond to different values of λ are given in table 3. C_2 (not needed for the calculations reported below) varies in the range 0.55–0.75 for $\lambda = 0.2$–3.0). Note that C_3^{-1} is the range of the screened dipole potential in the metal. We shall refer to it as the surface screening length.

This dipole–electron interaction is supplemented by a short range contribution associated with the electron–atom interaction considered in ref. [1f], as will be discussed in more detail below.

In addition to the molecule electron interaction we need to specify the static surface potential between the incoming molecule and the solid ion cores which governs the molecular motion. This is taken to be of the form

$$V_{AM}(x_A) = D\left[\left(\frac{x_0}{x_A}\right)^9 - 3\left(\frac{x_0}{x_A}\right)^3\right], \tag{9}$$

representing a large distances ($X_A \gg X_0$) an attractive dipolar part and at shorter distances the molecule surface repulsion. Both D and x_0 are quite uncertain. The choice of x_0 for, e.g., the HCl/Li system is guided by our expectation that it should be smaller than the corresponding value for the Ar/Li system (8 a.u.) and larger than the sum of atomic radii of Cl and Li (4.5 a.u.). We have taken x_0 to be 5–6 a.u. in all our calculations. The binding energy $2D$ for NO on the Li and Al surface was taken as 0.2 eV (its value for the NO/Ag and NO/Pt systems). For HCl on these surfaces the value is expected to be higher. We have used both $2D = 0.2$ eV and $2D = 0.7$ eV for these calculations.

3. Review of the theoretical approach

The method of calculation has been described in detail in a former publication [1f]. Here we outline just its essential points. For a single electron in one dimension (with mass m, coordinate x, kinetic energy T_e and potential energy in the metal field $U_e(x)$) colliding with a molecule represented by a point

dipole (of mass m_A, coordinate x_A, kinetic energy T_A and potential energy in the presence of the metal $V_{MA}(x_A)$), the Hamiltonian is

$$H = T_e + T_A + U_e(x) + V_{MA}(x_A) + V_{Ae}(x, x_A), \tag{10a}$$

where V_{Ae} is the electron–atom interaction. In the semiclassical TDSCF scheme the equations of motion for the electron and the atom are

$$\frac{\partial \psi(x, t)}{\partial t} = -\frac{i}{\hbar}[T_e + U_e(x) + V_{Ae}(x - x_A(t)]\psi_e(x, t), \tag{10b}$$

$$m_A \ddot{x}_A = -\frac{V_{MA}(x_A)}{x_A} - \frac{\partial}{\partial x_A}\int dx\, \psi_e^*(x, t)\, V_{Ae}(x - x_A)\, \psi_e(x, t). \tag{11}$$

To solve eq. (10b) for the electron wavefunction $\psi_e(x, t)$, we write it in the form

$$\psi_e(x, t) = \int_{k=0}^{\infty} dk\, G_k(t - t_0) \exp\left[-\frac{i}{\hbar}E_k(t - t_0)\right] f_k(x), \tag{12}$$

where $f_k(x)$ are the stationary states of the electron in the metal

$$[T_e + U_e(x)] f_k(x) = E_k f_k(x), \tag{13}$$

and where for $G_k(t)$ we choose the ansatz

$$G_k(t) = \left[\frac{2C(t)}{\pi}\right]^{1/4} \exp\left\{-C(t)[k - k_0(t)]^2\right\}. \tag{14}$$

Within this ansatz the wavefunction is determined by the two functions $C(t)$ and $k_0(t)$ and by the parameter t_0. The time evolution of $C(t)$ and $k_0(t)$ is obtained by minimizing, at each time, the quantity

$$\int dx\, |H\psi_e - i\hbar\, \partial\psi_e/\partial t|^2$$

with respect to $\dot{C}(t)$ and $\dot{k}_0(t)$, keeping $C(t)$ and $k_0(t)$ fixed during this minimization. This procedure leads to equations of motion for the function $C(t)$ and $k_0(t)$ which are solved together with eq. (11). As in our previous work we now identify $U_e(x)$ as the model potential $V(x)$ of eq. (1). The explicit forms of the time evolution equations for $k_0(t)$ and $C(t)$ are given for this case by eqs. (19)–(28) of ref. [1f]. These equations are solved subjected to the following initial conditions: (a) For the molecule $x_A(t \to -\infty) \to \infty$ and $p_A(t \to -\infty) \to (2mE)^{1/2}$ (p_A being the momentum and E the incident energy). (b) For the electron $k_0(t \to -\infty) \to \sqrt{2m\mathscr{E}}$ ($\mathscr{E}$ is the electron's initial energy) and $C(t \to -\infty)$ can be taken as any positive real number such that $C^{-1/2}(t \to -\infty) \ll k_F$ (as discussed previously [1f], we have to take C finite for reasons of stability of the numerical procedure). In addition we have to choose the initial position x_0 of the electron wavepacket. For an unperturbed propagation x_0 is related to t_0 of eq. (12) by $x_0 = k_0 t_0$. Then, t_0 is the time elapsed from the beginning of the motion to when the wavepacket reaches the surface
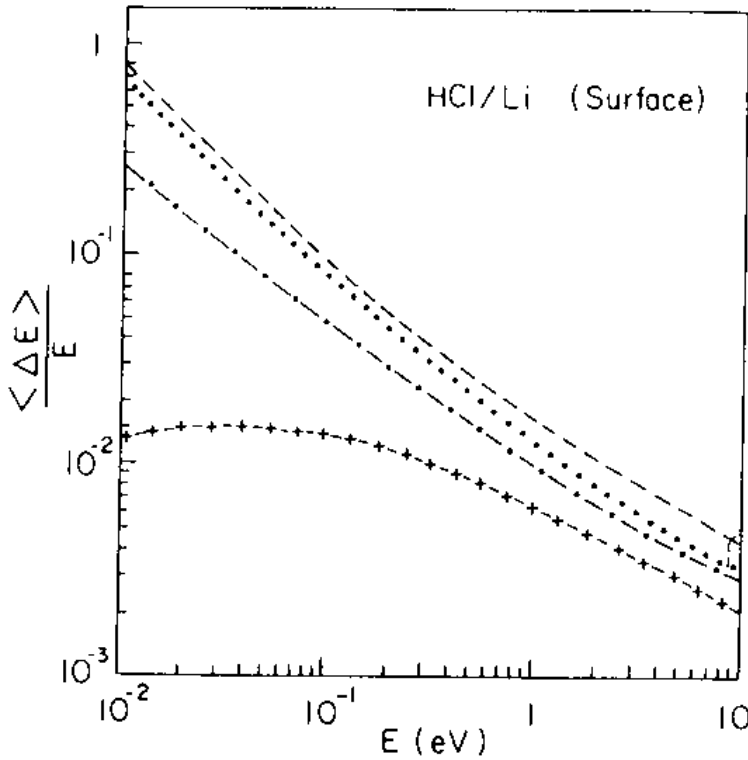
Fig. 1. Relative energy transfer $\langle \Delta E \rangle / E$ as a function of incident energy E for collision of HCl with a Li surface. Pure dipolar interaction is employed with the parameters C_1, C_2, C_3 and λ corresponding to the HCl/Li system. The values for D and x_0 are: (a) (dotted line) $D = 0.35$ eV, $x_0 = 6$ a.u.; (b) (dashed line) $D = 0.35$ eV, $x_0 = 5$ a.u.; (c) (dot-dashed line) $D = 0.1$ eV, $x_0 = 6$ a.u.; (d) (cross-dashed line) $D = 4.0 \times 10^{-3}$ eV, $x_0 = 7.2$ a.u. The parameters of curve (e) were employed for the He/Li system in ref. [1f].

$x = 0$. Given $\mathscr{E}$, x_0 and the somewhat arbitrary initial value of C_3, the numerical solution yields the energy transfer

$$E(\mathscr{E}, x_0) = \tfrac{1}{2} m_A \left[\dot{x}_A^2(t \to -\infty) - \dot{x}_A^2(t \to \infty) \right]$$

$$= \frac{\hbar^2}{2m} \left[k_0^2(t \to \infty) - k_0^2(t \to -\infty) \right].$$ (16)

The second part of eq. (16) is valid only provided $C^{-1/2}(t)$ remains much smaller than k_F throughout the collision process, otherwise $\hbar^2 k_0^2(t \to \infty)/2m$ has to be replaced by the final expectation value of the electronic energy. The total average energy transfer is then obtained using the relation [1f]

$$\langle \Delta E \rangle = \int d\mathscr{E} \int dx_0 f_T(\mathscr{E}) \left[1 - f_T(\mathscr{E}) + \Delta E(\mathscr{E}, x_0) \right] K(\mathscr{E}) \Delta E(\mathscr{E}, x_0),$$ (17)

where $K(\mathscr{E})$ is a weight function which we have taken [1f] to be

$$K(\mathscr{E}) = a^2 g(\mathscr{E}),$$ (18)

with $g(\mathscr{E})$ being the 3D one-electron density of states per unit volume and $a = (4\pi/3)^{1/3} r_s$. Eq. (17) is our final result to be reported below.

4. Results and discussion

In this section we report results of model calculations for energy transfer in collisions of NO and HCl molecules with Li and Al surfaces. In these calculations we have compared contributions of the long range dipolar part (eq. (8)) of the electron molecule interaction to that of the short range interaction which has been considered in a previous calculation [1f]. Note that in the calculation reported below, the surface temperature was taken to be zero.

Fig. 1 shows $\langle \Delta E \rangle / E$ as a function of the incident energy E where $\langle \Delta E \rangle$ is calculated from eq. (17) for a pure dipolar interaction (short range molecule–electron interaction disregarded) for several values of x_0 and D (eq. (9)) and with the parameters C_1, C_2, C_3 and λ from tables 1-3, which correspond to the HCl/L_i system. For comparison, the results for $2D = 4 \times 10^{-3}$ eV and $x_0 = 7.2$ a.u. (parameters for the He/L_i system), but for C and λ values and molecular mass corresponding to the HCl/L_i system, are also shown. These results are compared, in the same figure, to the energy transfer rate with a purely short range electron–molecule interaction. The short range interaction was taken to be a combination of hydrogen–electron and Ar-electron interactions employed in ref. [1f].

In fig. 2 we show the average relative energy transfer $\langle \Delta E \rangle / E$ for the

Table 2

Parameters for HCl and NO; m, l and μ are the mass, bond length and permanent dipole moment respectively

	m (a.u.)	l (a.u.)	μ (D)
HCl	37	2.40	1.07
NO	29	2.17	0.15

Table 3

Parameters for the electron–dipole interaction; λ is the Thomas–Fermi screening length, and C_1 and C_3 are defined by eq. (8)

λ (a.u.)	C_1 (a.u.)	C_3 (a.u.)
0.2	0.09	0.25
0.5	0.27	0.60
0.854 [a]	0.50 [a]	1.05 [a]
1.08 [b]	0.52 [b]	1.20 [b]
3.0	0.71	3.70

[a] Values derived from linearized Thomas–Fermi approximation for Li.
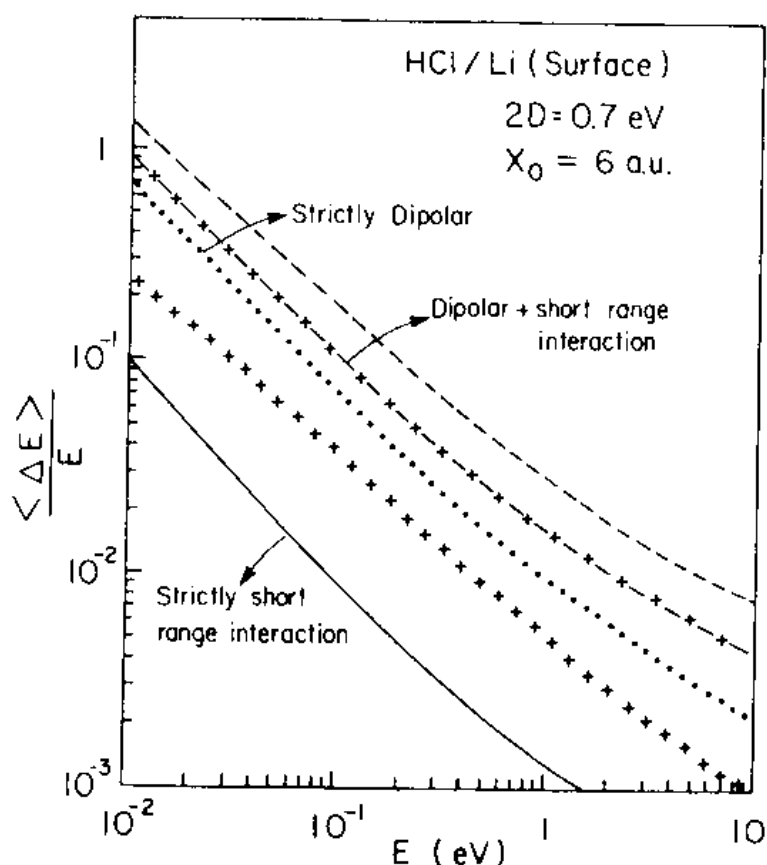[b] Values derived from linearized Thomas–Fermi approximation for Al.

Fig. 2. Relative energy transfer $\langle \Delta E \rangle / E$ as a function of incident energy E for the HCl/Li system. Short range and dipolar interaction are compared. All results are calculated with the following parameter values: $D = 0.35$ eV, $x_0 = 6$ a.u., and C_1, C_2, C_3 and λ corresponding to the HCl/Li system: (a) (full line) pure short range interaction, the same as in fig. 1; (b) (dotted line) pure dipolar interaction; (d) (dashed line) H atom facing the surface, dipolar and short range interaction reinforce each other; (d) (crossed line) Cl atom facing the surface, short range and dipolar interaction add destructively; (e) (cross-dashed line) combined short range and dipolar interaction, averaged over the two orientations.

HCl/Li system for the pure dipolar interaction ($D = 0.35$ a.u., $x_0 = 6.0$ a.u., C_1, C_3 and λ as in fig. 1) as well as for the combined short range and dipolar interactions. Again, the short range contribution is the combined Ar–electron and hydrogen–electron interaction as given in ref. [1f]. The upper curve in fig. 2 corresponds to a molecule approaching with the H atom facing the surface (attractive dipolar interaction which adds constructively to the short range interaction). The lower curve corresponds to a HCl molecule approaching with the Cl atom facing the surface, where the dipolar and short range interactions between the molecule and each electron add destructively. The average of ΔE over these two orientations is higher than that obtained by using the dipolar interaction alone. Note that an average relative energy transfer higher than 1 occurs when the strength of the static molecule–surface interaction is much higher than the incident energy. At such incident energies the static interaction potential governs the motion of the accelerated molecule near the surface. The amount of energy transfer can then also be greater than the total incident energy, leading to final negative energy states (trapping).
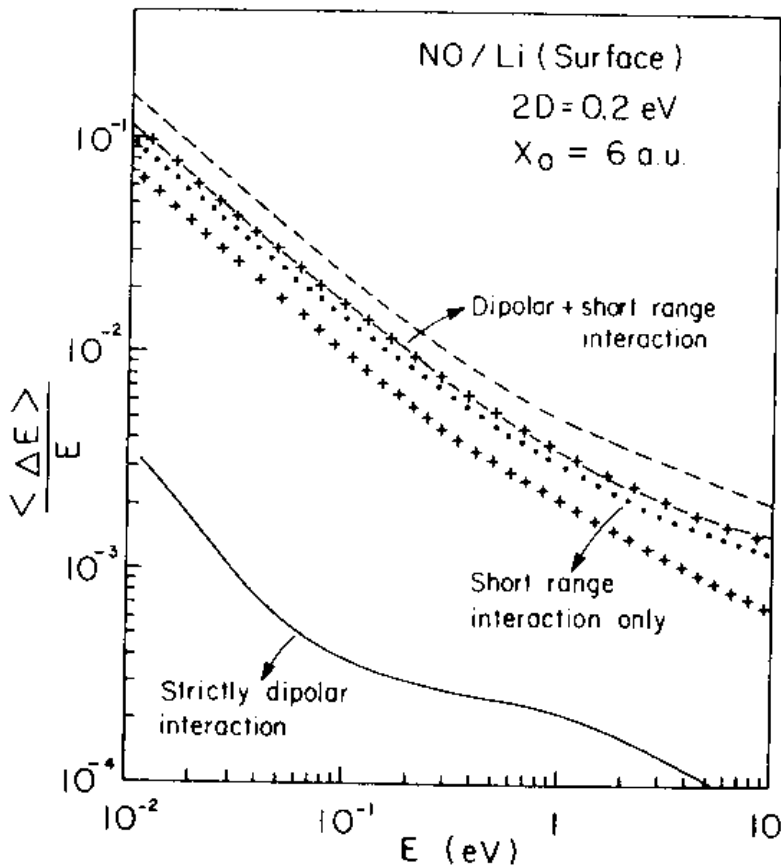
Fig. 3. Relative energy transfer $\langle \Delta E \rangle / E$ versus incident energy E for the NO/Li system. Results shown are calculated with the following parameter values: $D = 0.1$ eV, $x_0 = 6$ a.u., and C_1, C_2, C_3 and λ corresponding to the NO/Li system: (a) (dotted line) pure short range interaction; (b) (full line) pure dipolar interaction; (c) (dashed line) N atom facing the surface, short and long range interactions add constructively; (d) (crossed line) O atom facing the surface, short and long range interaction add destructively; (e) (cross-dashed line) combined short and long (dipolar) interaction, averaged over the two orientations.

Similar results for the NO/Li system are shown in fig. 3. The parameters of the dipolar interaction for this system are given in tables 1–3. For the short range interaction we took

$$V_{\text{short range}} = -0.23 \left[e^{-0.2(x_A - 1/2l - x)^2} + e^{-0.2(x_A + 1/2l - x)^2} \right],$$

where l is the molecule length given in table 2. The choice of this form is based on the effective electron–atom potentials calculated by Green et al. [4] which were fitted to an attractive Gaussian form following the same considerations as in ref. [1f]. The two contributions in the expression for V correspond to the electron interactions with the O and the N atoms. As in fig. 2, the average relative energy transfer for the combined short range and dipolar interaction is shown separately for the two orientation of the molecule (either N or O atom facing the surfaces) together with the average other the two orientations, compared to energy transfer due to purely dipolar and purely short range interaction. We see that the energy transfer in the NO/Li system is dominated
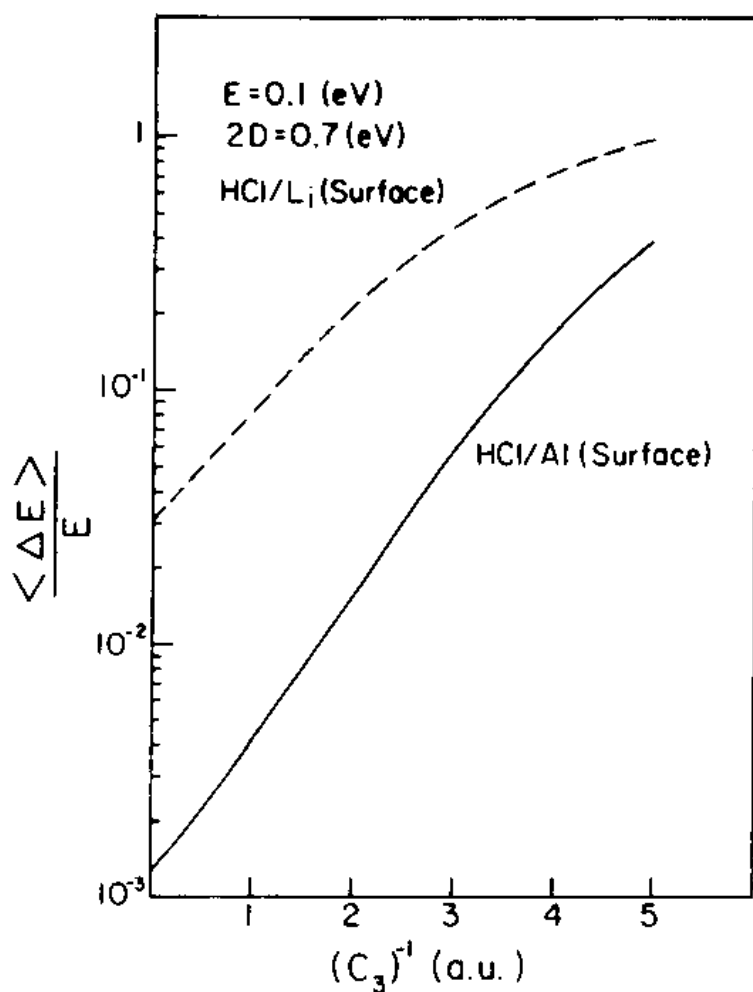
Fig. 4. Relative energy transfer $\langle \Delta E \rangle / E$ as a function of the surface screening length $(C_3)^{-1}$ of eq. (8) for the HCl/Li and HCl/Al system for a fixed initial energy $E = 0.1$eV and $D = 0.35$ eV, $x_0 = 6$ a.u. Only the dipolar long range interaction is employed. Values of C_1, depend on C_3 as shown in table 3: (a) (full line) HCl/Al system; (b) (dashed line) HCl/Li system.

by the short range interaction. In the HCl/Li system the dipolar interaction is dominant as seen in fig. 2, due to the strong dipole moment of HCl.

In fig. 4 we compare the energy transfer (plotted as a function of the surface screening length $(C_3)^{-1}$ of eq. (8)) for collision of HCl with Li and Al surfaces. The results seem fairly sensitive to the screening employed. At the same time we note that the results are also sensitive to several parameters characterizing the metal, in particular the work function. In this figure only the dipolar interaction was employed.

It is seen that energy transfer to Li is a much more efficient process than energy transfer to Al even though Al has a considerably greater electron density. The reason for that is, obviously, that as the work function of Li is lower than that of Al the Li electrons are much more effectively coupled to external perturbations.

Finally in fig. 5 we show the trapping probability vs. collision energy for collision of HCl, NO and hydrogen with Li surface. Separate trapping probability curves are shown for each of the two orientations of the incident HCl
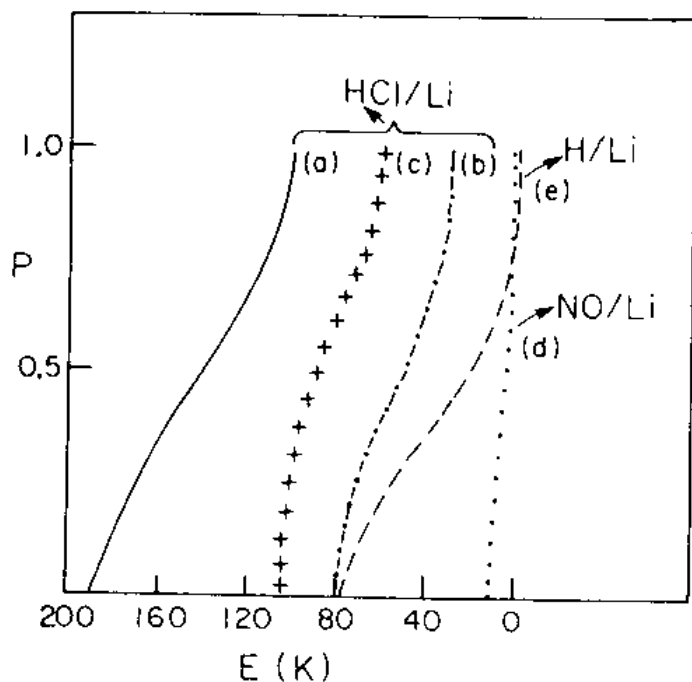
Fig. 5. Trapping probability for HCl, NO and hydrogen colliding with Li surface. Shown are: (a) (full line) HCl/Li collision, hydrogen facing the metal. $D = 0.35$ eV, $x_0 = 6$ a.u.; (b) (dotted dashed line) HCl/Li collision, Cl atom facing the metal, $D = 0.35$ eV, $x_0 = 6$ a.u. (the same values as in (a)); (c) (crossed line) HCl/Li collision, hydrogen facing the metal $D = 0.1$ eV, $x_0 = 6$ a.u.; (d) (dotted line) NO/Li collision, N atom facing the metal, $D = 0.1$ eV, $x_0 = 6$ a.u.; (e) (dashed line) H/Li collision, $D = 1.8$ eV, $x_0 = 3$ a.u.

molecule (either hydrogen or Cl atom is facing the metal) for $= 0.35$ eV.

Trapping efficiency appears to be strongly effected by the orientation of the dipolar molecule. Trapping takes place in considerably higher collision energies when the positive pole is facing the metal, due to the stronger total electron–molecule interaction in this case (short range and dipolar electron–molecule interactions add constructively) with ensuing increase in energy transfer and enhanced trapping effect. It should be kept in mind that in realistic situations all orientations of the incident molecule in 3D space are considered and the total trapping probability should be an average of the two limiting curves ((a) and (b)) in fig. 5 which correspond to the two perpendicular positions of the HCl molecule.

Trapping probability with the positive pole facing the metal were repeated for HCl/Li and NO/Li systems for $D = 0.1$ eV in both cases. For comparison we also show trapping probability of hydrogen colliding with Li surface ($D = 1.8$ eV) which appears in fig. 6 of ref. [1f].

Collisional energy transfer between an atom or a molecule and the free electron states of a metal is governed by several factors. These are the incident energy, the metal electron density (or equivalently the metal Fermi energy), the metal work function and the interaction potential. The latter is made of two parts which are taken as independent within our framework. The static interaction (determined in our model by the parameters D and x_0 of eq. (9))

governs the motion of the incident molecule near the surface. The electron-molecule interaction makes a relatively small contribution to the force exerted on the molecule by the metal but, phonons disregarded, it is responsible for the energy exchange between the metal and the molecule.

The calculations reported here demonstrate that for molecules with strong permanent dipole moments colliding with metal surfaces, the long range dipole-electron interaction, even though it is screened in the metal, can play a dominant role in the energy transfer process. It should be kept in mind however that the existence of permanent dipole moments affects not only the dynamic (electron-molecule) interaction but also the static molecule surface interaction (namely the parameters D and x_0 of eq. (9) within our model). As seen from figs. 1 and 2, the parameters affecting the static interaction have a profound effect on the energy transfer at low incident energies. This is of course mainly a manifestation of the higher effective collision energy associated with the larger well depth. Still the role played by the long range dynamic interaction is significant as seen by the strong dependence of the energy transfer on the magnitude of the dipole moment for the same static potential parameters as seen in figs. 1 and 2.

In summary, long range coulombic forces induced by an incident molecule carrying a permanent dipole moment may result in large energy exchange between the molecule and the metal electrons. Molecules carrying large dipole moments are expected to lose kinetic energy efficiently to a metal surface both because of the large well depth of the static molecule surface interaction associated with such molecules and because of the long range nature of the dynamic molecule-surface coupling.

Acknowledgements

References

[1] (a) R. Brako and D.M. Newns, J. Phys. C14 (1981) 305;
    (b) J.N. Gadzuk and H. Metiu, Phys. Rev. B22 (1980) 2603;
    (c) H. Metiu and J.W. Gadzuk, J. Chem. Phys.74 (1981) 2641;
    (d) K. Schonhammer and U. Gunnarson, Z. Physik 38 (1980) 127;
    (e) O. Gunnarson and K. Schonhammer, Phys. Rev. B25 (1982) 2514;
    (f) Z. Kirson, R.B. Gerber, A. Nitzan and M.A. Ratner, Surface Sci. 137 (1984) 527.
[2] D.M. Newns, J. Chem. Phys. 50 (1969) 4572.
[3] The result for E is found not to be sensitive to this value if it is taken small enough.
[4] A.E.S. Green, D.L. Sellin and A.S. Zachor, Phys. Rev. 184 (1969) 1.
    A.E.S. Green, D.L. Sellin and G. Darewych, Phys. Rev. A3 (1971) 169.